

Effect of the Mn clustering in (GaMn)N on the magnetic transition temperature

L. M. Sandratskii and P. Bruno

Max-Planck Institut für Mikrostrukturphysik, D-06120 Halle, Germany

S. Mirbt

Department of Physics, Uppsala University, Uppsala, Sweden

(Received 9 September 2004; revised manuscript received 2 November 2004; published 21 January 2005)

(GaMn)N is a topic of much current controversy. Rao and Jena suggested [Phys. Rev. Lett. **89**, 185504 (2002)] that a high Curie temperature detected in some of the (GaMn)N samples is a result of the formation of small Mn clusters carrying giant magnetic moments. We report a detailed density-functional-theory study of the effect of the Mn clustering on the electronic structure, exchange interactions, and Curie temperature in (GaMn)N. In contrast to the prediction, the Curie temperature decreases with the formation of the clusters. The main reason for this decrease is the splitting of the impurity band because of the intracluster Mn—Mn interaction that results in a decreased double-exchange effect. Additionally, the clustering increases the sensitivity of the magnetic properties with respect to the compensating defects.

DOI: 10.1103/PhysRevB.71.045210

PACS number(s): 75.50.Pp, 71.15.Mb, 75.30.Et

I. INTRODUCTION

The vision of semiconductor spin-electronics attracts immense experimental and theoretical attention to the design of the materials suitable for the realization of effective spin-injection into a semiconductor at room temperature. Among the requirements for these materials is a Curie temperature well above room temperature. After the detection of the ferromagnetism of (GaMn)As with the Curie temperature as high as 110 K,¹ the diluted magnetic semiconductors (DMS) are considered as one of the most promising classes of materials. Despite intensive efforts, the Curie temperature of (GaMn)As samples could not, however, be increased above 160 K.²

The prediction by Dietl *et al.*³ of the high- T_c ferromagnetism in (GaMn)N induced numerous experimental studies on this system. High Curie temperatures up to 940 K were, indeed, detected by a number of groups.⁴ On the other hand, some experimental groups question the ferromagnetism of (GaMn)N even in the low-temperature ground state.⁵

Also on the theoretical side, the character of the magnetic state in (GaMn)N is a matter of debate. Dietl *et al.* used as the basis for their prediction the Zener model that assumes the mediation of the magnetism by the semiconductor states.³ On the other hand, other researchers⁶ argue that to understand the magnetism of the III-V DMS, the double-exchange model based on a physical picture of the d -electron hopping between atoms with strong on-site Hund's exchange must be invoked.

An alternative to the model-Hamiltonian approaches is the density-functional-theory (DFT) calculations that intend to treat systems in their detailed complexity. In the realistic DFT calculations, different types of exchange interactions intermix and influence each other. Because of this generality, the DFT methods are able to describe the systems with various types of exchange interactions and are well suited for the investigation of this controversial material.^{7,8}

One of the very important, but up to now weakly studied, issues in the magnetism of DMS is the role of the impurity

clustering. Recently, Rao and Jena⁹ presented the DFT calculations of the nitrogen-doped Mn clusters and formulated an interesting hypothesis that explains a very high- T_c ferromagnetism observed in some of the (GaMn)N samples. The hypothesis is based on the assumption of the formation in (GaMn)N of small Mn clusters carrying giant magnetic moments. The giant cluster moments are assumed to interact strongly and, therefore, to be the reason for the high Curie temperature.

In this paper, we report a detailed DFT study of the influence of the Mn clustering on the magnetism of (GaMn)N. We confirm the assumption of Rao and Jena concerning the formation of giant cluster moments. We show, however, that the effect of the Mn clustering on the Curie temperature is opposite to the effect predicted.

II. CALCULATIONAL RESULTS AND DISCUSSION

The calculations are based on the supercell approach where one or several Ga atoms in a supercell of the semiconductor crystal are replaced by Mn atoms. Two types of the impurity patterns are considered. The first is a uniform pattern with one Mn atom per supercell. The second is a clustered pattern where two, three, or four Mn impurities per supercell replace, respectively, two, three, or four Ga atoms in the vertices of the Ga tetrahedron formed by the nearest neighbors of an N atom. All calculations of the clustered systems are performed for the $2a \times 2a \times 2a$ supercell, where a is the lattice parameter of the zinc-blende structure. To refer to different systems, we will use the notation of a p cluster, where $p=1,2,3,4$ is the number of impurities per supercell. The parameter p will be referred to as the size of the cluster.

First, we study the influence of the impurity clustering on the electronic structure of the ferromagnetically ordered (GaMn)N. Then, the stability of the ferromagnetic state is investigated by calculating Heisenberg's exchange parameters and the Curie temperature.

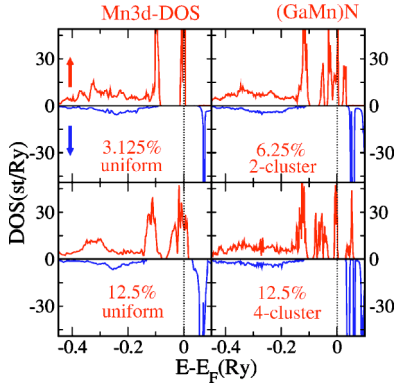


FIG. 1. (Color online) Mn 3d DOS.

The calculated values of the Mn atomic moment depend weakly on both Mn concentration and clustering and vary in a narrow interval, from $3.37\mu_B$ to $3.43\mu_B$. Therefore, the magnetic moment of the cluster is roughly proportional to the size of the cluster and for the four-cluster case has a large value of $13.72\mu_B$. This large value is in correlation with the prediction by Rao and Jena. However, the conclusion about the formation of giant cluster moments is justified only in the case in which the thermodynamics of the system can be described in terms of cluster moments. For this condition to be satisfied, the thermal fluctuations of the relative directions of the Mn atomic moments belonging to the same cluster must be much smaller than the fluctuations of the relative directions of the atomic moments belonging to different clusters. This problem will be addressed below.

A. Density of states

In Fig. 1, the calculated Mn 3d DOS is shown. First we compare two uniform Mn distributions with $x=3.125\%$ and $x=12.5\%$. The characteristic feature of (GaMn)N is the group of the Mn 3d spin-up states that form the impurity band in the energy region of the semiconducting gap. The comparison of the uniform impurity distributions shows that the main result of the increased concentration is, in this case, the broadening of the peaks of the DOS. This broadening reflects an increased interaction between impurity states with decreasing distance between nearest impurity atoms.

The clustering of the Mn atoms leads to a strong change in the character of the impurity band that is now split into several parts (Fig. 1). To understand the physical origin of the splitting caused by the clustering, we consider in Fig. 2 the partial 2p DOS of N atoms for (GaMn)N with $x=3.125\%$ (one-cluster case). The nitrogen atoms neighboring to the Mn impurities contribute strongly to the impurity-band states. This reveals strong Mn 3d–N 2p hybridization of the neighboring Mn and N atoms. On the other hand, the N 2p contribution into the impurity band decays strongly with increasing distance of the N atom from the Mn impurity. The spatial decay is characteristic for the impurity states lying in the semiconducting gap.

The following explanation of the splitting of the impurity band with clustering can now be suggested. The spatial closeness of the Mn atoms belonging to the same cluster and

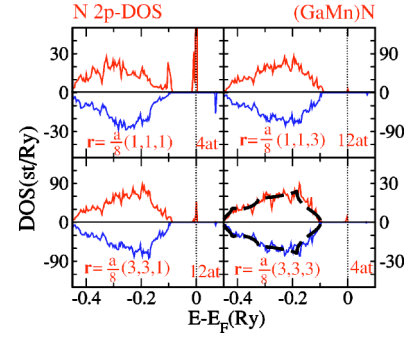


FIG. 2. (Color online) N 2p DOS for $x=3.125\%$. The vectors connecting the Mn atom with one of the N atoms of a given coordination sphere and the number of atoms in the sphere are shown. DOS is given per coordination sphere. The broken line in the bottom-right panel shows the semiconductor valence band.

strong Mn 3d–N 2p hybridization with neighboring nitrogen atoms lead to a strong effective interaction between the Mn 3d states within the cluster. Like in a molecule, the degenerate atomic levels split as a result of the interatomic intracluster interactions. The number of subgroups of the energy levels and the energy distances between them have a tendency to increase with increasing number of interacting atoms. Because of the spatial decay of the states, the broadening through the intercluster interaction is not sufficient to merge the levels split by the intracluster interaction in one group. These features of the electron structure are crucial for the understanding of the character of the Mn–Mn exchange interactions.

B. Exchange parameters and Curie temperature

To estimate the parameters of the interatomic exchange interactions, we map the results of the DFT calculations on an effective Heisenberg Hamiltonian of classical spins,

$$H_{\text{eff}} = -\frac{1}{N} \sum_{(mv) \neq (m'v')} j_{mm'}^{\nu\nu'} \mathbf{e}_m^\nu \cdot \mathbf{e}_{m'}^{\nu'}, \quad (1)$$

where ν, ν' label the Mn sublattices and m, m' label the cells. We use the calculational scheme based on the frozen-magnon approach as described earlier.¹⁰ A frozen-magnon state is characterized by a certain wave vector \mathbf{q} . Calculating the total energies of the frozen-magnon states for a regular \mathbf{q} mesh, one obtains Fourier transforms of the exchange parameters. The back-Fourier transformation gives Heisenberg's exchange parameters.

For the clustered systems considered in the paper, the determination of the exchange parameters consists of two steps. In the first step, the frozen-magnon calculations are performed for cluster moments. In the second step, the frozen-magnon calculations are done for one of the Mn sublattices. These two calculations give the exchange interactions between, respectively, cluster moments and the atomic moments belonging to one sublattice. Since all p Mn sublattices are equivalent, these calculations are sufficient for determining the Heisenberg exchange parameters in the system.

TABLE I. Calculated exchange parameters (mRy).

	cluster size (p)		
	2	3	4
j_0^{intra}	3.45	7.68	4.56
j_0^{inter}	0.48	0.125	0.03

In the mean-field approximation, the effective exchange fields acting on a given Mn moment from the Mn atoms outside of the given cluster and from the Mn atoms belonging to the same cluster are determined by the parameters

$$j_0^{\text{inter}} = \frac{1}{p} \sum_{m \neq 0} \sum_{vv'} j_{0m}^{vv'}, \quad j_0^{\text{intra}} = \frac{1}{p} \sum_{v \neq v'} j_{00}^{vv'}. \quad (2)$$

The calculated values of the exchange parameters are collected in Table I. The ferromagnetic intracluster exchange is in agreement with previous estimations of this quantity.^{7,9} Much stronger intracluster ferromagnetic exchange interaction compared to the intercluster interactions allows us to treat the thermodynamics of the system in terms of the rigid giant cluster moments. The Curie temperature of the system can be estimated as

$$k_B T_C^{\text{MF}} = \frac{2}{3} p j_0^{\text{inter}}. \quad (3)$$

The result of the calculation of the Curie temperature (Fig. 3) is opposite to that predicted by Rao and Jena: the clustering of the Mn atoms leads to a strong decrease of the Curie temperature. The Curie temperature drops not only compared with a uniform distribution of the same number of impurities, it also has a puzzling trend to decrease with the replacement of single impurities by impurity clusters.

C. Interpretation in terms of double-exchange and superexchange effects

An interpretation of the results of realistic DFT calculations is complicated by the complexity of the many-band interactions inherent for the DFT approach. Therefore, to explain this result it is useful to, first, discuss the influence of the frozen magnons on the total energy within the simple

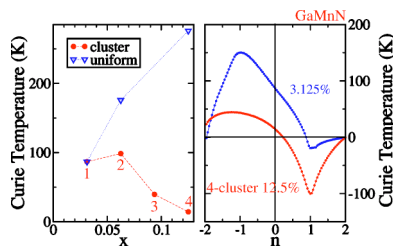


FIG. 3. (Color online) Left panel: The Curie temperature as a function of the Mn concentration. Numbers at the calculated points show the size of the clusters. Right panel: The Curie temperature as a function of the band occupation. $n=0$ corresponds to the nominal number of electrons.

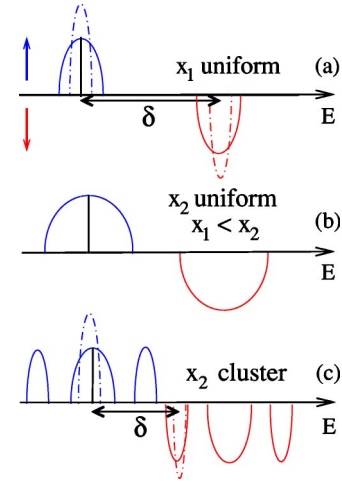


FIG. 4. (Color online) Schematic picture of the DOS of the impurity band for two Mn concentrations x_1 and x_2 ($x_1 < x_2$). The vertical solid lines show the position of the Fermi level. Comparison of (a) and (b) shows the band broadening with increasing concentration of the uniformly distributed defects. Comparison of (b) and (c) demonstrates the splitting of the band caused by the impurity clustering. The broken lines in (a) and (c) illustrate the effect of the deviation of the atomic moments from parallel directions that consists in the narrowing of the bands (double-exchange effect) and the shift of the centers of the gravity of the bands caused by the hybridizational repulsion. The magnitude of the shift increases with decreasing distance δ between the partially filled spin-up band and the lowest empty spin-down band. Therefore, the value of the anti-ferromagnetic superexchange is larger in case (c) than in case (a).

tight-binding model. The schematic picture in Fig. 4 helps to relate the properties of the simple model to the features of the realistic DFT calculations (Figs. 1 and 3). (The three panels in Fig. 4 correspond to the uniform Mn distributions with concentrations of 3.125% [panel (a)] and 12.5% [panel (b)] and the four-cluster case [panel (c)].)

In its physical essence, the mechanism of the effective positive exchange interaction in (GaMn)N is similar to the mechanism of the double exchange.¹¹ The strong exchange splitting of the Mn 3d states makes occupation of the Mn 3d spin-down states energetically unfavorable. One isolated energy band in an exchange field generated by a frozen-magnon magnetic configuration is described within a tight-binding approximation¹⁰ by the expression $\cos^2(\theta/2)\varepsilon(\mathbf{k} - \frac{1}{2}\mathbf{q}) + \sin^2(\theta/2)\varepsilon(\mathbf{k} + \frac{1}{2}\mathbf{q}) - (\Delta/2)$, where $\varepsilon(\mathbf{k})$ is the nonmagnetic band and Δ is the exchange splitting. The deviation of the atomic moments from parallel directions leads to the narrowing of the band keeping the position of the center of gravity unchanged (see Fig. 4 and its caption). If the band is empty or completely filled, the change of the magnetic configuration does not change the contribution of this band, to the total energy. For a partially filled band, the total energy of the occupied states increases with increasing noncollinearity that gives a positive (ferromagnetic) contribution to the interatomic exchange.

In contrast to the double exchange, the superexchange is essentially a many-band mechanism. The simple Anderson's formula for the superexchange $J = -b^2/\delta$ (Ref. 12) is, in its

essence, a standard second-order perturbation expression for the energy of a nondegenerate level, where δ is the energy distance to the first excited state and b is a small parameter describing the efficiency of the interlevel interaction caused by the perturbation. The expression is always negative since the interaction takes the form of the hybridizational repulsion where the lower level is bonding and decreases its energy. The consideration of two tight-binding bands in a frozen-magnon field shows that the hybridizational repulsion caused by a frozen magnon takes place also in this case.¹⁰ If the lower state is occupied and the upper state is empty, the repulsion decreases the energy of the system and gives negative (antiferromagnetic) contribution in the interatomic exchange parameters.

The energy increase caused by the double-exchange mechanism depends on the width of the partially filled band and the degree of the occupation of this band. On the other hand, the negative superexchange contribution depends on the energy distance between interacting states and the overlap of their wave functions.

In the case of a uniform impurity distribution, the width of the impurity band increases with increasing Mn concentration. For any impurity concentration there is one hole per Mn atom. This results in a monotonous increase of the interatomic exchange interactions and Curie temperature with increasing Mn concentration (Fig. 3).

In the clustered case, instead of one broader feature there is a group of separated impurity subbands. The ferromagnetic interaction caused by the double-exchange effect comes from the partially occupied subband. The width of the partially occupied subband tends to decrease with increasing cluster size (Figs. 1 and 4). Simultaneously, the splitting leads to a decrease in the number of holes per Mn atom in the partially filled subband. For example, the number of hole states per Mn atom in the four-cluster case is one-fourth of the corresponding number for the one-cluster case. Both the decrease of the width of the partially filled band and the decrease of the number of holes per Mn atom lead to a decreased double-exchange effect producing the trend to lower Curie temperature.

To elucidate the role of the superexchange, we performed a calculation of the interatomic exchange parameters and the Curie temperature as a function of the band occupation (Fig. 3). The value of $n=1$ corresponds to the situation where all energy bands are either completely filled or empty. The negative values of $T_c(1)$ reveal prevailing antiferromagnetic interactions in agreement with the concept of antiferromagnetic superexchange through completely occupied bands. The increase of $T_c(n)$ with deviation from $n=1$ either to higher or to lower n values confirms that partial occupation of the bands gives a ferromagnetic contribution to interatomic exchange interactions. The value of $[T_c(0) - T_c(1)]$ providing an estimation of the positive contribution to the interatomic ex-

change caused by the partial filling of the band is similar in both cases. Therefore, the reason for a lower T_c value in the four-cluster system is a more negative $T_c(1)$ that can be related to the decreased distance between hybridizing spin-up and spin-down states (Figs. 1 and 4).

Another important effect of the clustering is an increased dependence of the Curie temperature on the presence of uncontrolled donor defects. Indeed, the compensation of 10% of the holes changes, in the four-cluster case, the intercluster exchange from ferromagnetic to antiferromagnetic (Fig. 3). Since the number of holes is already decreased by the band splitting, this level of compensation is very low. This effect can be one of the reasons for nonferromagnetic or low- T_c states obtained experimentally for some of the (GaMn)N samples.

D. Concluding remarks

Concluding, we briefly comment on the difference between (GaMn)N and (GaMn)As. In (GaMn)As, the impurity band merges with the valence band, which leads to a much slower spatial decay of the states. As a result, the effect of the clustering on the Curie temperature in (GaMn)As is much weaker. This property correlates with a much smaller scattering of the experimental Curie temperatures in the case of (GaMn)As.

Note that the calculations presented in the paper were performed for unrelaxed atomic positions of the semiconductor matrix. The replacement of Ga atoms of a bulk semiconductor by Mn atoms is not expected to lead to a substantial lattice relaxation.¹³ To verify the validity of this expectation, we performed the calculation of the atomic relaxation for the four-cluster case. We used a plane-wave pseudopotential code [VASP (Refs. 14 and 15) within the local spin-density approximation (LSDA) (Ref. 16)]. The atoms are described by ultrasoft Vanderbilt-type pseudopotentials¹⁷ as supplied by Kresse and Hafner.¹⁸ The wave functions are expanded with an energy cutoff of 348 eV. The electron density was calculated using special k -point sets¹⁹ corresponding to a $2 \times 2 \times 2$ folding. The calculations were started with nonsymmetric positions of the Mn atoms. After the relaxation, the tetrahedral symmetry of the ideal Ga positions has been restored.

To study the sensitivity of the calculational results to the positions of the Mn atoms, we repeated the calculations of the four-cluster system for assumed inward and outward atomic relaxations up to 10% of the linear cluster size. Even for these very large changes of the Mn positions, all the conclusions of the paper remain qualitatively valid.

ACKNOWLEDGMENTS

The financial support of Bundesministerium für Bildung und Forschung is acknowledged.

- ¹H. Ohno, *Science* **281**, 951 (1998).
- ²D. Chiba, K. Takamura, F. Matsukura, and H. Ohno, *Appl. Phys. Lett.* **82**, 3020 (2003); K. W. Edmonds, P. Bogusawski, K.Y. Wang, R.P. Campion, S.N. Novikov, N.R.S. Farley, B.L. Gallagher, C.T. Foxon, M. Sawicki, T. Dietl, M. Buongiorno Nardelli, and J. Bernholc, *Phys. Rev. Lett.* **92**, 037201 (2004).
- ³T. Dietl, H. Ohno, F. Matsukura, J. Cibert, and D. Ferrand, *Science* **287**, 1019 (2000).
- ⁴S. Sonoda, S. Shimizu, T. Sasaki, Y. Yamamoto, and H. Hori, *J. Cryst. Growth* **237**, 1358 (2002); N. Theodoropoulou, A. F. Hebard, M. E. Overberg, C. R. Abernathy, S. J. Pearton, S. N. G. Chu, and R. G. Wilson, *Appl. Phys. Lett.* **78**, 3475 (2001); M. L. Reed, N. A. El-Masry, H. H. Stadelmaier, M. K. Rittums, M. J. Reed, C. A. Parker, J. C. Roberts, and S. M. Bedair, *Appl. Phys. Lett.* **79**, 3473 (2001).
- ⁵S. Dhar, O. Brandt, A. Trampert, L. Däweritz, K. J. Friedland, K. H. Ploog, J. Keller, B. Boschoten, and G. Güntherodt, *Appl. Phys. Lett.* **82**, 2077 (2003).
- ⁶P. M. Krstajic, F. M. Peeters, V. A. Iuanov, V. Fleurov, and K. Kikoin, e-print cond-mat/0311525.
- ⁷M. van Schilfgaarde and O. N. Mryasov, *Phys. Rev. B* **63**, 233205 (2001).
- ⁸K. Sato, P. H. Dederichs, H. Katayama-Yosida, J. Kudrnovsky, *Physica B* **340**, 363 (2003); L. Kronik, M. Jain, and J. R. Chelikowsky, *Phys. Rev. B* **66**, 041203 (2002); B. Sanyal, O. Bengone, and S. Mirbt, *ibid.* **68**, 205210 (2003); A. Filippetti, N. A. Spaldin, and S. Sanvito, e-print cond-mat/0302178; P. Mahadevan and A. Zunger, *Phys. Rev. B* **69**, 115211 (2004); L. M. Sandratskii, P. Bruno and J. Kudrnovský, *ibid.* **69**, 195203 (2004).
- ⁹B. K. Rao and P. Jena, *Phys. Rev. Lett.* **89**, 185504 (2002).
- ¹⁰L. M. Sandratskii and P. Bruno, *Phys. Rev. B* **66**, 134435 (2002); **67**, 214402 (2003).
- ¹¹P. W. Anderson and H. Hasegawa, *Phys. Rev.* **100**, 675 (1955); H. Akai, *Phys. Rev. Lett.* **81**, 3002 (1998).
- ¹²P. W. Anderson, *Phys. Rev.* **115**, 2 (1959).
- ¹³G. P. Das, B. K. Rao, and P. Jena, *Phys. Rev. B* **68**, 035207 (2003); S. Mirbt, B. Sanyal, and P. Mohn, *J. Phys.: Condens. Matter* **14**, 3295 (2002).
- ¹⁴G. Kresse and J. Hafner, *Phys. Rev. B* **47**, RC558 (1993).
- ¹⁵G. Kresse and J. Furthmüller, *Phys. Rev. B* **54**, 11 169 (1996).
- ¹⁶D. M. Ceperley and B. J. Alder, *Phys. Rev. Lett.* **45**, 566 (1980).
- ¹⁷D. Vanderbilt, *Phys. Rev. B* **41**, 7892 (1990).
- ¹⁸G. Kresse and J. Hafner, *J. Phys.: Condens. Matter* **6**, 8245 (1994).
- ¹⁹H. J. Monkhorst and J. D. Pack, *Phys. Rev. B* **13**, 5188 (1976).